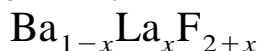




# Inelastic neutron scattering study of the superionic solid solutions



F. Kadlec<sup>a, b,\*</sup>, F. Moussa<sup>c</sup>, P. Simon<sup>a</sup>, B.P. Sobolev<sup>d</sup>

<sup>a</sup>CNRS–CRPHT, 45071 Orléans Cedex 2, France

<sup>b</sup>Institute of Physics, Academy of Science Czech Republic, 180 40 Prague 8, Czech Republic

<sup>c</sup>Laboratoire Léon Brillouin (CEA–CNRS), CEN Saclay, 91191 Gif sur Yvette, France

<sup>d</sup>Institute of Crystallography, Academy of Science of Russian Federation, 117 333 Moscow, Russia

---

## Abstract

Inelastic neutron scattering spectra of  $\text{Ba}_{1-x}\text{La}_x\text{F}_{2+x}$  single crystals have been measured at temperatures from 450 to 1000°C. A noticeable result at  $x = 0.16$  consists in a low-energy inelastic mode ( $E = 0.8$  THz) which is observed at a specific wavevector only and takes the form of a quasielastic signal for other wavevectors. This is explained by the assumption that the mode comprises mobile ions and defect clusters; the characteristic wavevector corresponds to the short-distance correlation length between the clusters. For  $x = 0.31$ , this mode seems overdamped, which we explain by enhanced interactions between the clusters. © 1999 Elsevier Science B.V. All rights reserved.

*Keywords:* Inelastic neutron scattering; Superionic conductivity; Localized modes; Fluorite structure

---

## 1. Introduction

In recent years, the fluorite-structured solid solutions with the general formula  $(\text{MF}_2)_{1-x}(\text{RF}_3)_x$  ( $M = \text{Ca}, \text{Sr}, \text{Ba}, \text{Pb}$  and  $R$  is a rare-earth element or  $Y$ ) have been the subject of numerous experimental studies focused on their superionic properties. It is known that the doping of  $\text{MF}_2$  by trivalent  $R$  elements substantially enhances the disorder and ionic conductivity  $\sigma$  (see, e.g., [1,2]). The overall cubic crystal symmetry (space group  $Fm\bar{3}m$ ) is conserved up to  $x \leq x_{\text{max}}$  where  $x_{\text{max}} \approx 0.4$ – $0.5$  depending on  $M, R$  [3]. As in the pure fluorite

structure crystals, the conductivity is due to hopping of mobile  $\text{F}^-$  anions.

On doping in the order of units of per cent or more, the crystal defects gather into clusters, the structure of which depends, in general, on  $M$  and  $R$  [4,5]. The lattice in the vicinity of the clusters is deformed, which leads to so-called defect regions [6] surrounded by the undeformed fluorite lattice. According to the Enhanced Ionic Motion model [7], these deformations are supposed to enhance  $\sigma$  by locally decreasing the value of the activation enthalpy for hops of  $\text{F}^-$  ions, instead of by increasing the proportion of mobile ions. This provides an easy conduction path for them in the closest vicinity of the clusters. In agreement with this model it has been found experimentally, at least for two systems, that

---

\*Corresponding author. Fax: +420-2-821227.

E-mail address: kadlec@fzu.cz (F. Kadlec)

the concentration of charge-carrying ions is independent of  $x$  [8,9].

Evidence of the cluster structure and configuration in the  $(\text{BaF}_2)_{1-x}(\text{LaF}_3)_x$  single crystals has been obtained by diffuse neutron scattering (DNS) [10,11]. The main conclusions were as follows:

- The clusters in this system are of the 2:2:2 type.
- The clusters form aggregates which comprise clusters aligned along the  $\langle 100 \rangle$  directions. At room temperature, there are on average four clusters per aggregate. Within the aggregate, the distances between cluster centres are  $3a/2$  along the aggregate axis and  $a/2$  in one of four perpendicular  $\langle 100 \rangle$  directions. The directions of these transverse displacements are random.
- On heating, the mean number of clusters involved in the aggregates decreases as the aggregates decompose into individual clusters. The most significant drop is observed between 500 and 750°C; this interval coincides with an anomalous increase in  $\sigma$ . The authors suggest that the short range cluster correlations affect the conductivity.

The presence of low-energy excitations in  $(\text{BaF}_2)_{1-x}(\text{LaF}_3)_x$  corresponding to the model of two-level systems [12] has been suggested earlier [13] on the basis of low temperature thermal conductivity, specific heat and internal friction measurements. It has been found that features characteristic for glasses and amorphous solids develop with increasing  $x$ . Similarly, signs of possible localized vibrational excitations known from disordered solids have been established in the Raman spectra [14].

In the present article, we report results of inelastic neutron scattering (INS) experiments which yield, for the first time, direct information about the dynamics of the clusters. Our results strongly support the idea about the close relationship between the conductivity mechanism and the short-range correlations.

## 2. Experimental

The single crystalline samples were grown from melts by the Bridgman technique [15] under fluorinating atmosphere at the Institute of Crystal-

lography, Moscow. They had the form of parallelepipeds with a size of  $6 \times 6 \times 4 \text{ mm}^3$ . The doping rate  $x$  has been verified within  $\pm 0.5\%$  by means of an electron microprobe connected to an electron microscope.

INS experiments were performed at the reactor Orphée in the Laboratoire Léon Brillouin, Saclay on the triple-axis spectrometer 4F2 installed at a cold neutron source. Pyrolytic graphite crystals were used as monochromator and analyser. The samples with doping rates  $x = 0.16$  and  $x = 0.31$  were mounted in a high-vacuum aluminium furnace using a niobium sample holder and heated at temperatures from 450°C to 1000°C. The scans were performed at a fixed scattered wave vector of  $|\mathbf{k}_f| = 2.662 \text{ \AA}^{-1}$  and momentum transfer  $\mathbf{Q} = [2 \ 2 \ -q_l]$ . This choice of scattering geometry mainly permits analysis of vibrations which are transverse with respect to  $\mathbf{q}$ .

## 3. Results and evaluation

### 3.1. $(\text{BaF}_2)_{0.84}(\text{LaF}_3)_{0.16}$

The INS spectra of the  $x = 0.16$  sample obtained at 600°C are shown by symbols in Fig. 1. In all graphs, positive energy corresponds to phonon creation. The scale of the y-axis was chosen in order to show the inelastic part of the spectra in detail. The experimental data were fitted using a procedure which takes into account the characteristics of the apparatus. The spectra were taken at constant monitor counting rate.

Fig. 1a shows the spectrum obtained at the Brillouin zone point  $\mathbf{q} = [0 \ 0 \ 0.4]$ . The inelastic part has been fitted using three Lorentzian curves: (1) a broad quasielastic term with half-width at half maximum (HWHM)  $\Gamma = 3.5 \text{ THz}$ ; (2) a phonon at  $E = 1.4 \text{ THz}$  and  $\Gamma = 0.12 \text{ THz}$  and (3) a weak phonon at  $E = 2.7 \text{ THz}$ . (Note: In Fig. 1a, this feature is not evident but the peak has been detected at the same position in all the spectra at higher temperatures (see Fig. 2).) The contributions of these terms are shown by dashed lines, together with those of the background noise and the elastic signal. The sum of all contributions is shown by a solid line.

At  $\mathbf{q} = [0 \ 0 \ 0.6]$ , the spectral shape is rather different (Fig. 1b): in order to fit the experimental

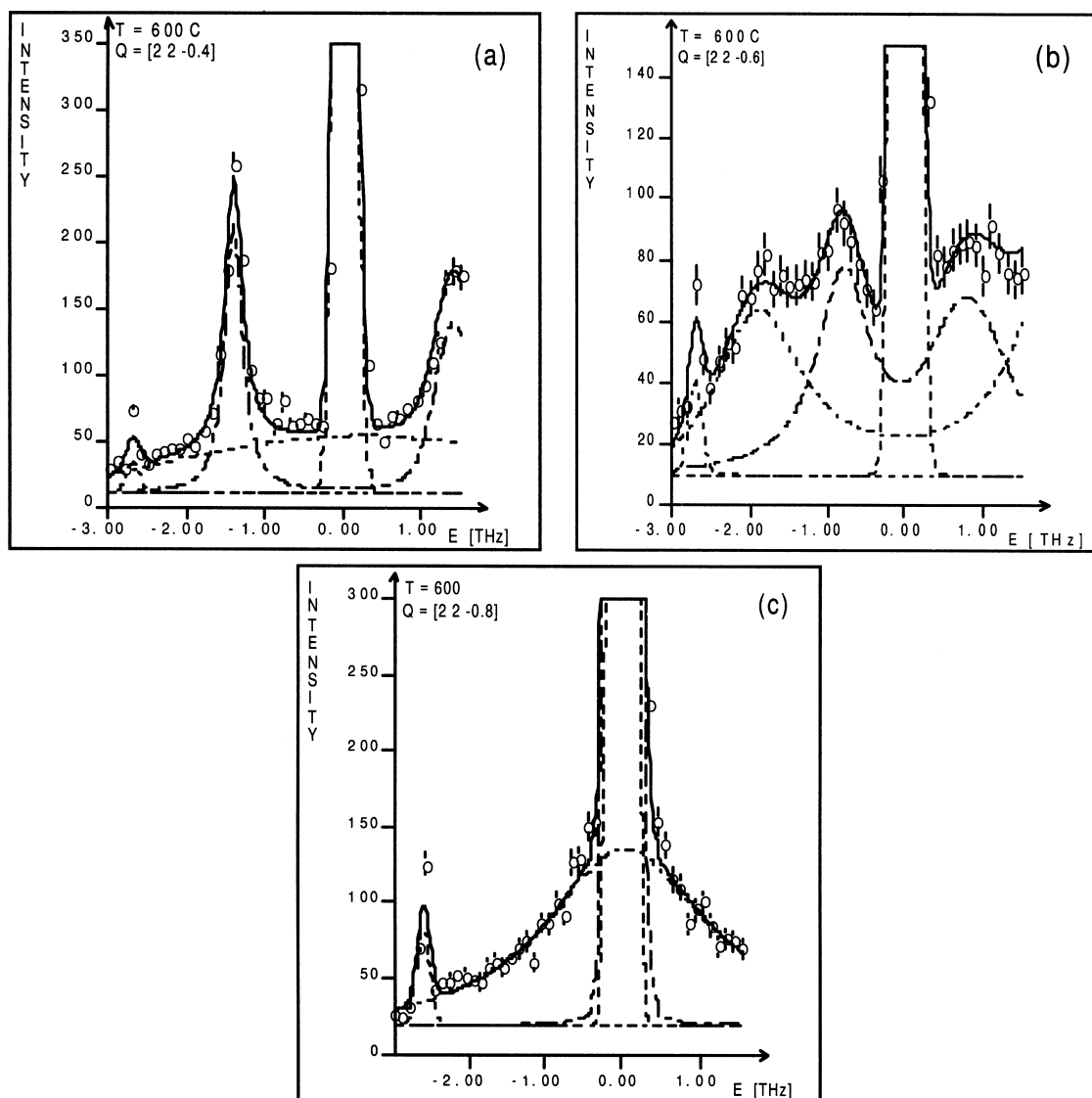


Fig. 1. INS spectra of  $(\text{BaF}_2)_{0.84}(\text{LaF}_3)_{0.16}$  at  $T = 600^\circ\text{C}$ ,  $\mathbf{q} = [0\ 0\ q_1]$ : (a)  $q_1 = 0.4$ , (b)  $q_1 = 0.6$ , (c)  $q_1 = 0.8$ ; experimental data are shown by symbols and fits by solid lines.

points, three underdamped well-defined modes are necessary. Their parameters are, respectively:  $E = 0.8$  THz and  $\Gamma = 0.4$  THz;  $E = 1.9$  THz and  $\Gamma = 0.6$  THz;  $E = 2.7$  THz and  $\Gamma \approx 0.1$  THz.

Finally, at  $\mathbf{q} = [0\ 0\ 0.8]$ , apart from the elastic peak, only two contributions are clearly present (see Fig. 1c): a broad quasielastic term with  $\Gamma = 1.2$  THz and the narrow peak with  $E = 2.6$  THz,  $\Gamma \approx 0.1$  THz.

On further heating, the scattered intensity increases due to the Bose–Einstein factor increase; the main features of the spectra are conserved. At  $\mathbf{q} = [0\ 0\ 0.4]$ , softening and broadening of the TA mode can be observed (see Fig. 2). While the softening is more or less continuous,  $\Gamma$  rises the most steeply between 800 and 900°C (see Fig. 3). On the other hand, there are no signs of softening of the peaks at  $E = 2.7$  THz at any value of  $q_1$ .

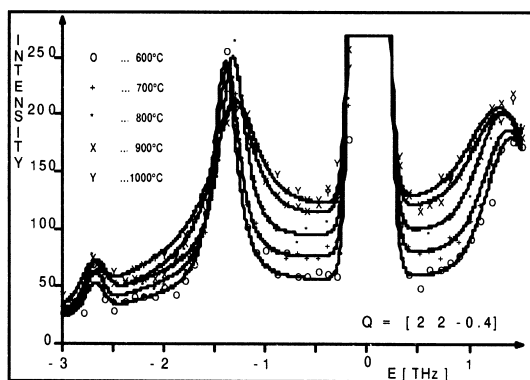


Fig. 2. Temperature dependence of the INS spectra of  $(\text{BaF}_2)_{0.84}(\text{LaF}_3)_{0.16}$  at  $\mathbf{q} = [0\ 0\ 0.4]$ .

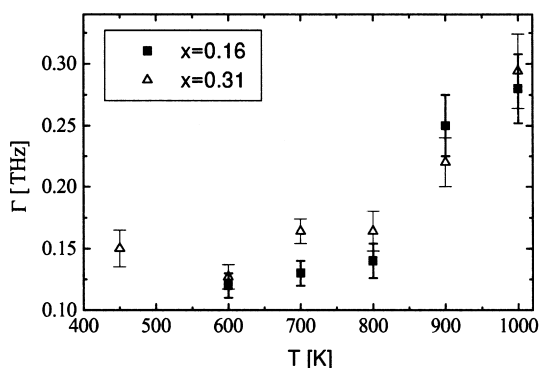


Fig. 3. Temperature dependence of the TA peak width at  $\mathbf{q} = [0\ 0\ 0.4]$ .

### 3.2. $(\text{BaF}_2)_{0.69}(\text{LaF}_3)_{0.31}$

The INS spectra in the  $\mathbf{q} = [0\ 0\ q_l]$  direction (see Fig. 4) were measured at the same points of the Brillouin zone as in the  $x = 0.16$  doped sample. Due to a different geometry of the sample mounting, the spectra could be measured in the energy interval  $-2\ \text{THz} \leq E \leq 1.5\ \text{THz}$  only for  $q_l = 0.4, 0.6$  and within  $-2\ \text{THz} \leq E \leq 0.5\ \text{THz}$  for  $q_l = 0.8$ . Therefore, we could not check for the presence of the mode at  $E \approx 2.7\ \text{THz}$ .

The spectra obtained at  $q_l = 0.4, 0.8$  are qualitatively the same as in the  $x = 0.16$  sample: a broad quasielastic signal and peaks due to the TA mode can be seen (see Fig. 4a, c). However, in this case, the same holds for  $q_l = 0.6$  (see Fig. 4b); thus, the spectrum differs significantly from that of the  $x =$

0.16 sample, as no peak has been observed near  $E = 0.8\ \text{THz}$ .

On heating, we have also observed softening and broadening of the TA phonon at  $\mathbf{q} = [0\ 0\ 0.4]$  (see Fig. 5); compared to the  $x = 0.16$  sample, the increase of  $\Gamma$  above  $800^\circ\text{C}$  is slower (see Fig. 3).

## 4. Discussion

### 4.1. $(\text{BaF}_2)_{0.84}(\text{LaF}_3)_{0.16}$

On the basis of the room-temperature phonon dispersion curves, it is possible to compare the transverse acoustic (TA) branch of  $\text{BaF}_2$  [16] with the positions of the inelastic peaks (see Fig. 6). Thus, we can assign to the TA mode the peak at  $1.4\ \text{THz}$  in Fig. 1a, as well as that at  $1.9\ \text{THz}$  in Fig. 1b. The interpretation of the peak at  $2.6\ \text{THz}$  in Fig. 1c is not completely clear. Its position corresponds well to that of the TA branch in  $\text{BaF}_2$ , but it is much less intense and narrower than the TA peak at  $q_l = 0.4$  and  $0.6$ . Moreover, peaks with a similar energy, intensity and width have been observed in these spectra. Therefore we think that the TA phonon is broadened and not observable at  $q_l = 0.8$ ; this suggests that the peaks at  $E = 2.6\ \text{THz}$  belong to a dispersionless branch, probably corresponding to a localized excitation. Note that a similar branch attributed to a localized mode with the energy about  $E = 1.5\ \text{THz}$  has been reported earlier in Na  $\beta$ -alumina [17].

An even more surprising result is the change of the quasielastic peak observed at  $q_l = 0.4$  and  $q_l = 0.8$  into a mode at  $q_l = 0.6$  with a well-defined frequency. Our interpretation is based on the defect structure determined earlier ([11], see Section 1). The characteristic distance between clusters within one aggregate is  $d^* = 3a/2$  in the  $[0\ 0\ 1]$  directions [11]. Our DNS experiments [18] show that doping causes a local increase of the lattice parameter by about 11% within aggregates which was not taken into account in [11]. As the reciprocal space coordinates refer to the  $\text{BaF}_2$  matrix, it is necessary to replace  $a$  by  $1.11a$  in the above expression for  $d^*$  and one obtains  $d^* = 1.67a$ . We suppose there is a (localized) vibration along  $[0\ 0\ 1]$ , in which adjacent clusters move in antiphase. Then, the wavelength of

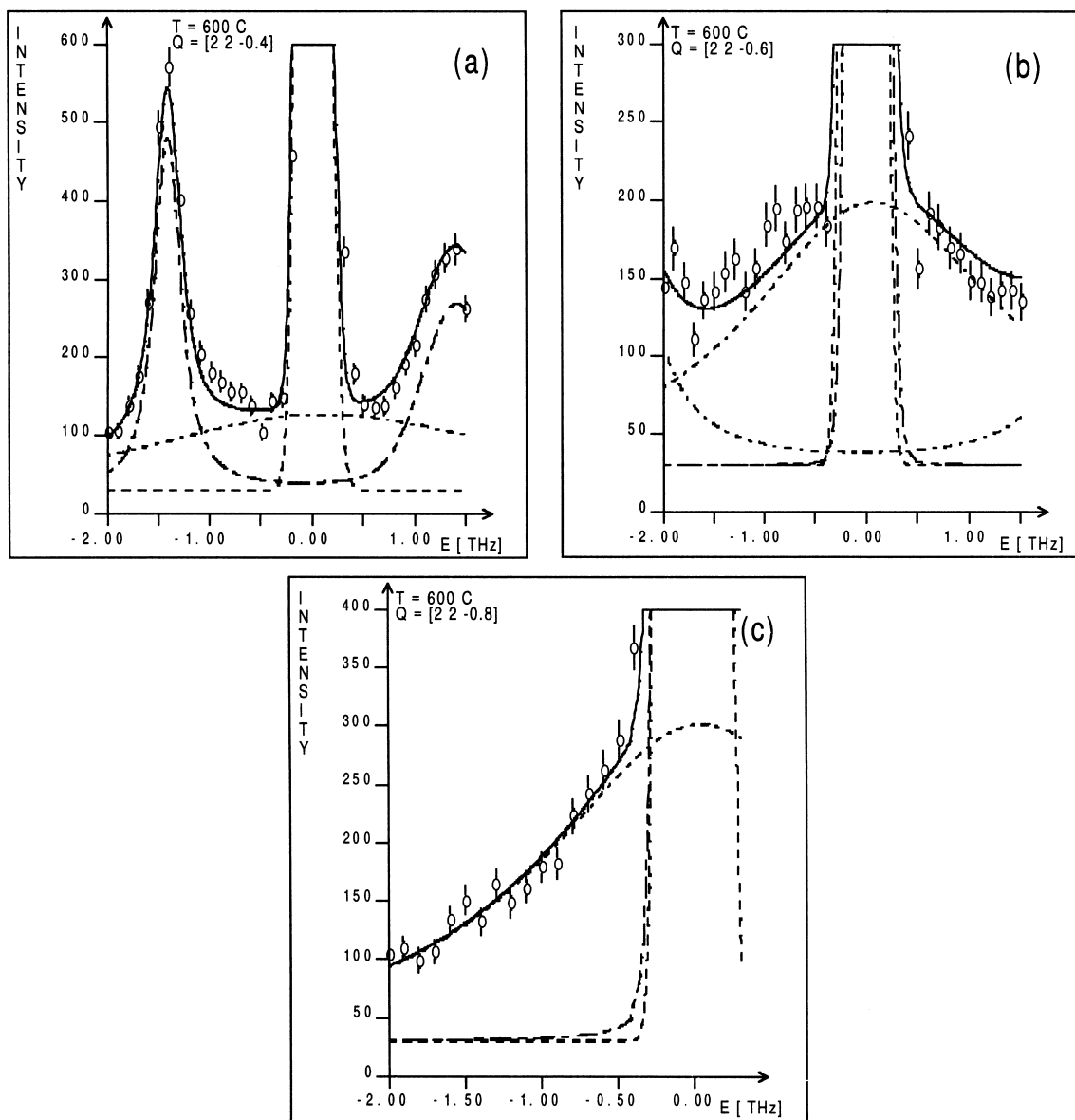


Fig. 4. INS spectra of  $(\text{BaF}_2)_{0.69}(\text{LaF}_3)_{0.31}$  at  $T = 600^\circ\text{C}$ ,  $\mathbf{q} = [0\ 0\ q_l]$ : (a)  $q_l = 0.4$ , (b)  $q_l = 0.6$ , (c)  $q_l = 0.8$ ; experimental data are shown by symbols and fits by solid lines.

such a vibration is  $\lambda^* = 2d^* = 3.33a$  and its wavevector  $\mathbf{q}^* = [0\ 0\ q_l^*]$  with  $q_l^* \equiv 2\pi/\lambda^* = 0.6\frac{\pi}{a}$ . If this interpretation is correct, the localized vibration of clusters interacts the most strongly with the ‘sea’ of mobile ions, present near the cluster surface, just at  $q_l = 0.6$ . So, the oscillation frequency  $E = 0.8$  THz is a result of local forces in the system of clusters

and mobile ions which are in resonance. At wavelengths sufficiently far away from this value, the incident neutron beam excites a strongly damped vibration only, which is why a large quasielastic term is observed.

We presume that the fast increase of the width of the TA mode between 800 and 900°C (see Fig. 3)

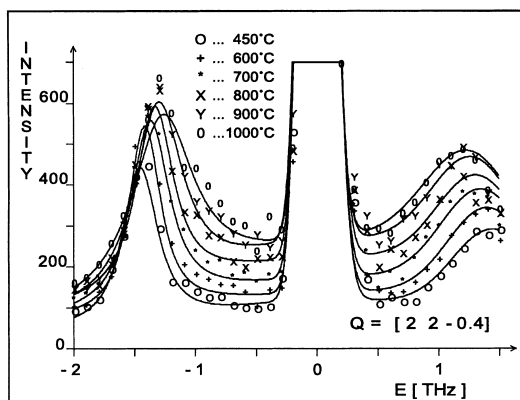


Fig. 5. Temperature dependence of the INS spectra of  $(\text{BaF}_2)_{0.84}(\text{LaF}_3)_{0.16}$  at  $q = [0\ 0\ 0.4]$ .

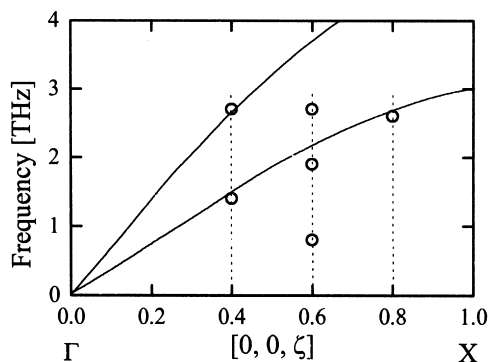


Fig. 6. Room temperature phonon dispersion curves of  $\text{BaF}_2$  (solid lines, [16]) and positions of inelastic peaks observed in  $(\text{BaF}_2)_{0.84}(\text{LaF}_3)_{0.16}$  at  $600^\circ\text{C}$  (open circles). The dotted lines mark constant  $Q$  scans performed on this sample.

shows the coupling of the TA mode to the mobile ions which change their dynamic behaviour with temperature. Note that this temperature region lies just above the marked deviation of  $\sigma$  from Arrhenius behaviour [19]. Another sign of such a coupling is the absence of the TA phonon at  $q_l = 0.8$ . The fact that the peaks at  $E \approx 2.7$  THz do not soften is in agreement with our assumption that they are due to another localized mode; besides, it shows that the changes of local force constants with temperature are negligible.

#### 4.2. $(\text{BaF}_2)_{0.69}(\text{LaF}_3)_{0.31}$

In the  $x = 0.31$  sample, the resonance effect which has been observed for  $x = 0.16$  is absent (cf. Fig. 1b

and Fig. 4b). This change in the lattice dynamics is undoubtedly due to higher doping. A possible explanation is that the increased concentration of clusters enhances dissipation forces between them, which can be observed especially well in this point of the Brillouin zone, where, at lower  $x$ , the lattice structure and dynamics are favourable for the resonance.

At temperatures up to  $800^\circ\text{C}$ , the width of the TA mode at  $q_l = 0.4$  is somewhat higher than for  $x = 0.16$  (see Fig. 3). This is in agreement with the idea of broadening due to an interaction between the TA branch and mobile ions: as their mobility is higher, the mode is broader. We cannot satisfactorily explain the fact that the increase in  $\Gamma$  above  $800^\circ\text{C}$  is slower than in the less-doped sample.

## 5. Conclusions

In  $(\text{BaF}_2)_{0.84}(\text{LaF}_3)_{0.16}$ , we have established the presence of an underdamped localized mode with  $E = 0.8$  THz, apparently involving both defect clusters and mobile  $\text{F}^-$  ions. We think that this mode can play an important role in the conductivity mechanism. Furthermore, another localized mode with a small dispersion presumably exists near  $E = 2.6$  THz. In  $(\text{BaF}_2)_{0.69}(\text{LaF}_3)_{0.31}$ , the former mode is, as we suppose, overdamped due to stronger interactions between the clusters. In order to confirm our assumptions, further INS experiments at similar values of  $q_l$  and  $x$  are foreseen.

## Acknowledgements

We would like to express our thanks to P. Boutrouille from LLB for technical support of the experiments and to K. Jurek from the Institute of Physics, Prague for establishing the exact doping rates.

## References

- [1] D. Grandjean, T. Challier, D.J. Jones, P. Vitse, Solid State Ionics 51 (1992) 297.
- [2] A.K. Ivanov-Shits, N.I. Sorokin, P.P. Fedorov, B.P. Sobolev, Solid State Ionics 31 (1989) 269.
- [3] B.P. Sobolev, Bull. Soc. Chém. XII (1991) 275.
- [4] J.M. Réau, P. Hagenmuller, Appl. Phys. A 49 (1989) 3.

- [5] S.V. Chernov, W. Gunßer, I.V. Murin, *Solid State Ionics* 47 (1991) 67.
- [6] A.K. Ivanov-Shits, N.I. Sorokin, P.P. Fedorov, B.P. Sobolev, *Solid State Ionics* 31 (1989) 253.
- [7] K.E.D. Wapenaar, J. Schoonman, *J. Electrochem. Soc.* 126 (1979) 667.
- [8] E.F. Hairetdinov, N.F. Uvarov, Y.J. Xu, J.M. Réau, *Physica Status Solidi (b)* 203 (1997) 17.
- [9] E.F. Hairetdinov, N.F. Uvarov, M. Wahbi, J.M. Réau, *Solid State Commun.* 101 (1997) 681.
- [10] N.H. Andersen, in: *6th Risø International Symposium On Metallurgy and Materials Science*, 1985, p. 171.
- [11] N.H. Andersen, K.N. Clausen, J.K. Kjems, J. Schoonman, *J. Phys. C: Solid State Phys.* 19 (1986) 2377.
- [12] W.A. Phillips, *Rep. Prog. Phys.* 50 (1987) 1657.
- [13] D.G. Cahill, R.O. Pohl, *Phys. Rev. B* 39 (1989) 10477.
- [14] M. Kolesík, D. Tunega, B.P. Sobolev, *Physica Status Solidi (b)* 160 (1990) 375.
- [15] A.K. Ivanov-Shits, N.I. Sorokin, B.P. Sobolev, P.P. Fedorov, *Fizika Tverdogo Tela* 25 (1983) 1748.
- [16] J.P. Hurrell, V.J. Minkiewicz, *Solid State Commun.* 8 (1970) 463.
- [17] S.M. Shapiro, F. Reidinger, in: M.B. Salomon (Ed.), *Physics of Superionic Conductors*, Springer Verlag, Berlin, 1979, p. 45.
- [18] F. Kadlec, P. Simon, F. Moussa, B.P. Sobolev, *Mat. Sci and Eng. B* 57 (1999) 234.
- [19] N.I. Sorokin, M.W. Breiter, *Solid State Ionics* 99 (1997) 241.